ELSEVIER

Thermochimica Acta 384 (2002) 57–69

thermochimica acta

www.elsevier.com/locate/tca

Hazard characterization of KDNBF using a variety of different techniques

D.E.G. Jones*, P.D. Lightfoot, R.C. Fouchard, Q. Kwok, A.-M. Turcotte, W. Ridley

Canadian Explosives Research Laboratory, 555 Booth Street, CANMET, Natural Resources Canada, Ottawa, Ont., Canada K1A 0G1

Abstract

New results are presented on the thermal stability of the primary explosive, the potassium salt of 4,6-dinitrobenzofuroxan (KDNBF) and on the mechanism of its decomposition. The new work complements and extends previous work done in our laboratory. The thermal decomposition of KDNBF has now been studied using a wide variety of experimental techniques: differential scanning calorimetry (DSC), thermogravimetric analysis (TGA), accelerating rate calorimetry (ARC), heat flow calorimetry (HFC) and simultaneous thermogravimetry–differential thermal analysis (TG–DTA). The latter technique is coupled in our laboratory to FTIR and mass spectrometers to provide a very powerful method where the reaction products, the mass change and the temperature difference between the sample and reference can be monitored simultaneously as the material is decomposed.

The results demonstrate that the decomposition takes place by a multi-step exothermic process directly from the solid state. The initial decomposition process does not appear to depend on the nature of the atmosphere, or the total pressure. The main gaseous product of the decomposition is carbon dioxide, with water, nitrous oxide and cyanogen also being formed.

Kinetic parameters measured for the decomposition using a number of different techniques are in good agreement over eight orders of magnitude. An average of the available data gives: $\ln(k/\mathrm{min}^{-1}) = (41.2 \pm 5.7) - ((170 \pm 22)\ \mathrm{kJ\ mol}^{-1})/RT$. Although sensible Arrhenius data were generated, it was demonstrated that the mechanism of the decomposition is far from simple. For example, if KDNBF is thermally aged, its onset temperature can be decreased significantly, demonstrating that substantial changes to the material can occur well below its apparent decomposition temperature. The sensitivity of KDNBF to impact, friction and electrostatic discharges was also established. The results are compared to those available in the literature for KDNBF and for other primary explosives.

Keywords: Thermal analysis; KDNBF; DSC; TG; TG–DTA–FTIR–MS

1. Introduction

The potassium salt of 4,6-dinitrobenzofuroxan (KDNBF) (Fig. 1) is more stable and less impact sensitive than the parent compound [1]. KDNBF has been used in primary explosive and initiator compositions since the early 1950s [2], with recent emphasis on its environmental advantages over materials that contain heavy metals [3,4]. Despite this continued interest in KDNBF, only limited information is available on its thermal properties.

Our laboratory has been interested in the thermal properties of KDNBF for several years. We have previously published or presented differential scanning calorimetry (DSC), thermogravimetry (TG), accelerating rate calorimetry (ARC) and heat flow calorimetry

* Corresponding author. Tel.: +1-613-995-2140; fax: +1-613-995-1230.
E-mail address: djones@nrcan.gc.ca (D.E.G. Jones).

0040-6031/02/$ – see front matter
PII: S0040-6031(01)00777-8

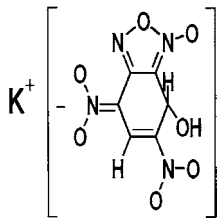

Fig. 1. Structure of potassium 4,6-dinitrobenzofuroxan.

(HFC) data on the thermal decomposition of KDNBF [5–8]. Apart from the earlier work in our laboratory, there has been little systematic work done on the thermal decomposition of KDNBF [9–14]. Our interest in KDNBF is both practical and fundamental. Firstly, there is limited information on the thermal hazards of this highly sensitive material. A better understanding of the thermal hazards of KDNBF should thus improve safety in manufacture and handling operations. Secondly, the material displays interesting behavior in that it appears to decompose directly from the solid state [5], facilitating the study of the reaction. A simple solid-state decomposition would potentially eliminate the complications of data interpretation inherent when phase changes and reactions between phases are present.

The present work complements and extends our previous studies. This paper presents the following new data.

1. Kinetic parameters by DSC, according to ASTM E698.
2. Identification of the gas-phase reaction products by FTIR and MS.
3. Kinetic parameters from the time dependence of product generation in isothermal experiments by TG–DTA–FTIR–MS.
4. Impact, friction and electrostatic sensitivity data.

The results are compared to those previously obtained by other methods in our laboratory and elsewhere.

2. Experimental

2.1. Materials

KDNBF from two sources was tested. The first batch was supplied by Stresau Laboratory Inc. and was shown by NMR measurements to be at least 99% pure. This material was used in our previous work on KDNBF [5–8] and for some of the TG–DTA work in the present study. A second sample of KDNBF was obtained from Eagle-Picher Industries Inc. This second sample, of unstated purity, was used for most of the work reported here. The close similarity of the results obtained for the two samples suggests that the two samples were of similar purity. No additional purification was conducted on either of the samples prior to their use in the experiments described below. Anti-static precautions were used when manipulating KDNBF. Conductive table mats, sample containers and wrist straps were used. The relative humidity in the room was also kept above 30%.

2.2. DSC

A TA Instruments 2910 DSC was used for these measurements. Dry, oxygen-free nitrogen was used to purge the DSC at $50\,cm^3\,min^{-1}$. Heating rates, β, from 1 to 10 °C min^{-1} were employed. Sample sizes were about 0.2 mg, contained in hermetically sealed aluminum pans. Temperature and heat flow calibrations using SRM standards were performed prior to the experiments [15].

2.3. TG

A TA Instruments 2950 TG instrument was used for the measurements reported here. Approximately 1 mg of sample was held in a platinum pan, in a flow of dry nitrogen ($100\,cm^3\,min^{-1}$, split 60:40 between the furnace and the balance). The sample was brought rapidly to the isothermal temperature of 100–125 °C and held there for several days. The TG instrument was calibrated for mass and temperature. The standard reference weight used for mass calibration was checked against a Mettler M3 microbalance with a precision of ± 1 μg. The temperature was calibrated using the Curie point magnetic method with SRM nickel [16].

2.4. TG–DTA–FTIR–MS

Simultaneous thermogravimetry–differential thermal analysis (TG–DTA) was carried out using a TA

Instruments SDT 2960 instrument, with evolved gas analysis using a Bomem MB100 FTIR spectrometer and a Balzers Thermostar GSD300 quadrupole mass spectrometer. The TG–DTA–FTIR–MS data were acquired simultaneously in one run. Approximately 1 mg of sample was placed in an alumina pan. The DTA reference material was ~1 mg platinum foil. The sample and reference were purged with 50 cm^3 min^{-1} of air or helium. Two types of TG–DTA experiments were performed. In the first, the temperature was ramped from ambient to 400 °C at 5 °C min^{-1} in an atmosphere of dry air or helium. In the second, the sample was heated rapidly to a chosen temperature and maintained isothermally in an atmosphere of dry air until reaction was complete.

The FTIR interface consists of a 5 mm i.d. Teflon tube and a 10 cm Pyrex cell with a 50 cm^3 volume and KBr windows. A quartz microfiber filter is placed at the FTIR inlet. The acquisition rate of the FTIR is every minute and the time delay is ~10 s from the TG–DTA furnace outlet to the FTIR cell. Bomem Grams 32 software was utilized for data acquisition and presentation.

The mass spectrometer data were acquired using the Balzers Quadstar 422 software. The heated quartz capillary interface was placed near the sample pan, in the TG–DTA furnace. Data were acquired using bar graph scan, programmed to acquire data from 1 to 120 amu (atomic mass unit) at a speed of 0.2 s amu^{-1}.

TG mass, DTA baseline and temperature calibrations (indium and tin) were performed prior to the experiments. Calcium oxalate was also run under the same conditions, as a final check on the system performance.

2.5. Impact apparatus

The bureau of explosives machine was used to determine the impact sensitivity of the KDNBF according to the procedure described in the UN Manual of Tests and Criteria [17]. The 3.63 kg mass was dropped onto the hardened steel sample assembly containing approximately 10 mg of KDNBF powder. A total of 25 drops were performed using a Bruceton up-and-down technique [18]. The height for 50% probability of ignition (H_{50}) and the standard deviation of the trials were calculated using Franklin Applied Physics Bruceton Analysis software.

2.6. Friction apparatus

The friction sensitivity of KDNBF was determined with the BAM Friction Apparatus according to instructions described in the UN Manual of Tests and Criteria [19]. The test was performed with a quantity of sample (approximately 10 mm^3) positioned between the porcelain peg and plate. A series of trials at different frictional loads were conducted to determine the limiting load or the lowest load in which at least one ''explosion'' occurred.

2.7. Electrostatic discharge sensitivity (ESD) apparatus

An ESD tester manufactured by Franklin Applied Physics was used to determine the electrostatic discharge sensitivity of KDNBF. The ESD tester was equipped with a 500 pF capacitor, a power supply capable of delivering up to 25 kV and a 5000 kΩ non-inductive discharge resistor. The sample cells consisted of #10 nylon washers glued to 12.7 mm diameter disks of 0.127 mm thick steel shimstock [20]. Approximately 0.030 cm^3 of KDNBF was loaded into each sample cell that was subsequently sealed with a strip of Scotch type 810 magic tape. The sample cells were placed on a grounded, brass sample cell holder. A brass electrode equipped with a replaceable, nickel-plated brass dressmaker pin (0.6 mm in diameter by 30 mm long) was lowered onto the sample cell until the tip of the pin perforated the tape membrane. The limiting energy for the ESD initiation of KDNBF was determined by subjecting the sample to sparks of varying energies.

3. Results

3.1. ASTM E698

Arrhenius parameters for the thermal decomposition of KDNBF were determined by DSC, using ASTM method E698 [21], which assumes first-order kinetics. Fig. 2 shows a typical DSC trace. There are at least three exothermic peaks in the trace, one strong initial peak, with two much weaker subsequent peaks. The kinetic analysis that follows was based on the first peak. Enthalpies of reaction were

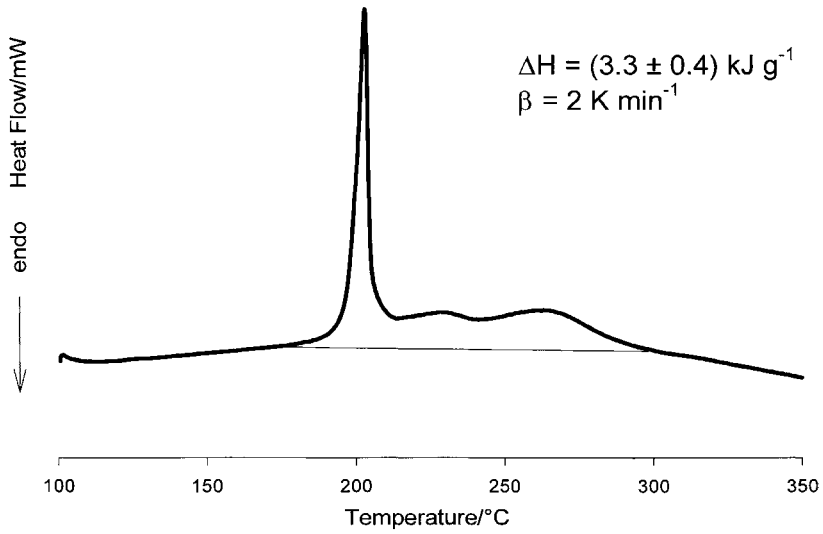

Fig. 2. Typical DSC trace: 0.205 mg KDNBF, 2 °C min^{-1}.

obtained by integrating over the whole decomposition, however.

The E698 method requires measurement of the dependence of the temperature at which the maximum heat generation is observed (T_c) on heating rate (β). The experimental results are summarized in Table 1. The average enthalpy of reaction is 3.3 ± 0.4 kJ g^{-1}. A plot of $\ln(\beta/T_c^2)$ against 10^3 K/T_c is shown in Fig. 3. The slope of the plot is equal to $-E/R$; the Arrhenius pre-exponential factor is derived as an average over all the experiments, based on the activation energy. Values of $\ln(Z/\text{min}^{-1}) = 42.7 \pm 0.1$ and $E/\text{kJ mol}^{-1} = 176 \pm 5$ were obtained.

ASTM E698 also requires that a half-life test be carried out to verify the kinetics. The Arrhenius parameters are used to calculate the temperature at which half of the material should react in 1 h (176 °C in the present case). The sample is then thermally aged for 60 min at that temperature and subsequently subjected to a regular, temperature-ramped DSC run after quenching. If the kinetic parameters are correct, the only change in the DSC results should be that the peak area (or peak height) for the aged sample is expected to be half that generated by a fresh sample. Fig. 4 shows DSC traces from a half-life test carried out at 176 °C and a heating rate of 10 °C min^{-1}. The peak height for the aged sample is close to that expected, but the onset temperature of the first peak is significantly reduced. In contrast, the positions of the second and third exothermic peaks are unchanged. Because of this unusual behavior, a number of isothermal experiments were carried out between 150 and 178 °C; the results are summarized in Table 2. In every case, the onset temperature of the aged sample was lower than that of the non-aged sample. No difference was observed between experiments in which the sample was quenched after the pre-heating and those where the sample was subjected to a temperature ramp directly from the aging temperature.

Average mass losses in DSC experiments were $60 \pm 9\%$. This value is close to that observed in

Table 1
Dependence of KDNBF DSC results on heating rate (ASTM E698)

Sample mass/mg	β/°C min^{-1}	T_c/°C	ΔH/kJ g^{-1}
0.202	1.01	198.0	2.82
0.192	1.01	196.5	3.11
0.205	2.02	203.0	3.84
0.205	2.02	203.0	3.79
0.207	5.07	212.7	2.91
0.227	5.07	212.1	3.43
0.223	10.18	220.7	3.29
0.242	10.10	220.4	3.03

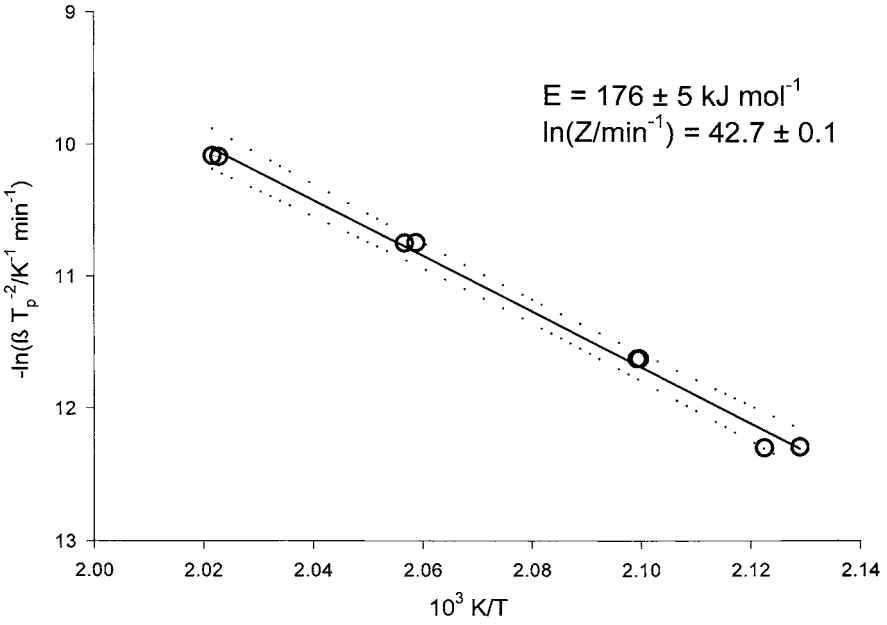

Fig. 3. Arrhenius parameters by ASTM E698: plot of $-\ln(\beta/T_c^2)$ vs. 10^3 K/T_c. Regression fit and 95% confidence intervals also shown.

open-pan TG–DTA experiments and demonstrates that, although the lids on the DSC pans were crimped, they could not contain the pressures generated during the decomposition.

3.2. TG

As is discussed later, there is a considerable discrepancy between an extrapolation of the present

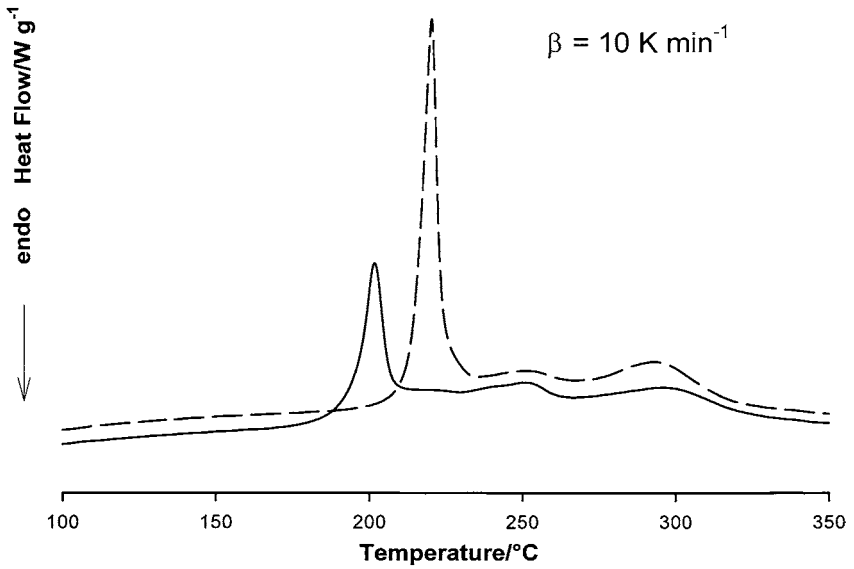

Fig. 4. Effect of isothermal aging on the thermal decomposition of KDNBF: solid line, with aging; dashed line, without aging.

Table 2
Results of isothermal aging experiments[a]

T_{iso}/°C	t_{iso}/min	Predicted fraction remaining	Measured fraction remaining	β/°C min^{-1} for temperature-ramp experiments	T_{max} measured/°C	T_{max} expected/°C
178.1	60	0.41	0.32	10	202.9	220.6
176.0	60	0.48	0.43	10	201.8	220.6
176.2	60	0.48	0.43	1	187.3	197.2
170.5	120	0.45	0.38	10	201.0	220.6
150	1440	0.38	0.68	5	196.0	212.4
150	1440	0.38	0.60	5	198.3	212.4

[a] Samples were heated at T_{iso} for a period of t_{iso}, then subjected to a standard DSC temperature-ramp procedure. Measured fractions remaining are based on the height of the first peak relative to that of unaged samples.

kinetic results and mass loss experiments reported by Rouch and Maycock [9]. In order to verify the present results at lower temperatures, several TG mass-loss experiment were conducted over the range 100–125 °C.

3.3. TG–DTA

The results of a typical, temperature-ramped TG–DTA run in dry air at a heating rate of 5 °C min^{-1} are shown in Fig. 5. The strong first exotherm is very clear in the DTA trace, with an accompanying mass loss. Experiments run in helium and air gave very similar results up to 250 °C, demonstrating that an oxidizing atmosphere does not affect the primary decomposition. When air was used as the purge gas, an additional exotherm and mass loss were observed between 350 and 400 °C, attributed to the oxidation of the carbonaceous residue.

A number of products were observed in the gas phase. The peak concentrations for all products coincided with the peak of the initial exotherm. The FTIR data in Fig. 5 are shown as absorbances, the MS data as ion currents. Although the FTIR and MS data are not calibrated for quantitative measurements, it is clear that carbon dioxide was the most significant product in the gas phase. Also observed were water vapor and nitrous oxide, in much smaller quantities.

The only product observed by MS, but not by FTIR was the very minor product cyanogen, $(CN)_2$. A late peak in the carbon dioxide absorbance was observed between 350 and 400 °C, when air was used as the carrier gas, confirming that oxidation of a carbonaceous residue is taking place. The solid residue in a helium atmosphere amounts to approximately 40% of the original mass. Limited analysis of the solid residue by FTIR, after heating 1 mg of KDNBF to 400 °C, indicated a complex mixture, with evidence for the existence of nitrate, nitrite, carbonate and C–N or azide species.

Typical traces, in isothermal TG–DTA experiments, of carbon dioxide absorbance as a function of time are shown in Fig. 6. In each case, heating to within a degree of the final isothermal temperature was achieved in less than 5 min. Once at the isothermal temperature, there is a delay before carbon dioxide begins to evolve. For most temperatures, a double peak in the carbon dioxide absorbance is observed. The peak absorbance increases and the time to the peak absorbance decreases with increasing temperature.

Kinetic information can be derived from an analysis of the time for a particular event to occur in isothermal studies [22]. Based on the assumption that the time for a particular event to occur is inversely proportional to the rate constant, the activation energy for a process can be derived from the slope of a plot of ln(time-to-event) against $1/T$. Fig. 7 shows such a plot for the carbon dioxide absorbance data: t_1 refers to the first peak in the carbon dioxide absorbance; t_2 refers to the second. The slopes from the two plots are very similar, giving activation energies of 152 ± 6 and 160 ± 5 kJ mol^{-1} for t_1 and t_2, respectively. The results for the two samples of KDNBF are very similar. The activation energy for the process can similarly be estimated from plots of ln(peak absorbance) versus $1/T$, assuming that the rate of reaction is proportional to the carbon dioxide concentration. Fig. 7 shows the data in this form. Again, there is excellent agreement

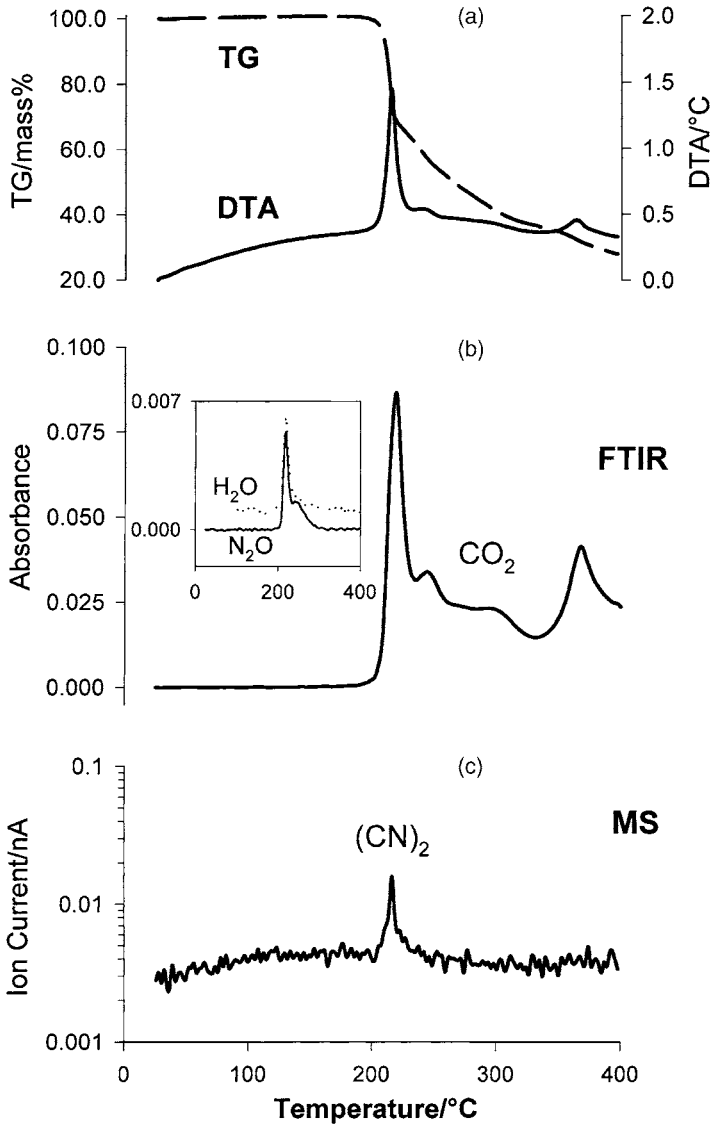

Fig. 5. TG–DTA–FTIR–MS run in air, showing (a) mass loss and temperature difference data by TG and DTA; (b) reaction products in the gas phase by FTIR spectrometry; (c) cyanogen in the gas phase by mass spectrometry $(m/z) = 52$.

between the results for the two samples of KDNBF. Analysis of the data gives activation energies of 173 ± 5 and 168 ± 8 kJ mol^{-1} for the first and second peak, respectively.

3.4. Sensitivity

The sensitivity data obtained in this work is summarised in Table 3. KDNBF is extremely sensitive to impact, friction and electrostatic discharges. The height of 50% probability of ignition (H_{50}) of the KDNBF was found to be 6.1 ± 1.3 cm. The limiting load for the initiation of KDNBF by friction in the BAM tests was found to be <5 N. KDNBF was ignited at the lowest energy available from the ESD tester (6 mJ). When positive reactions were observed, the material completely disappeared, with an accompanying loud report.

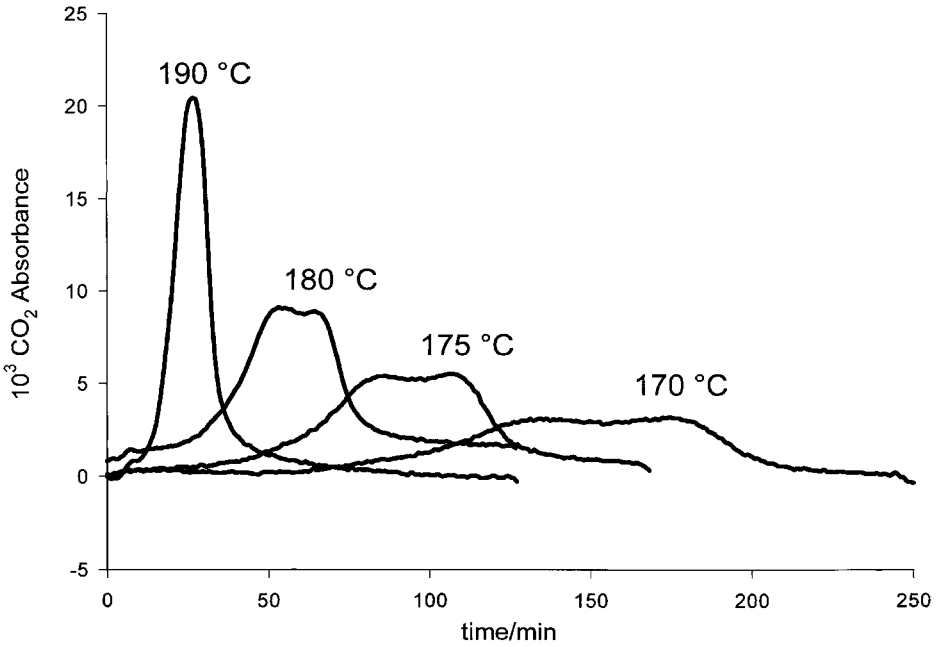

Fig. 6. Time dependence of carbon dioxide production in isothermal TG–DTA–FTIR–MS experiments in air at different temperatures.

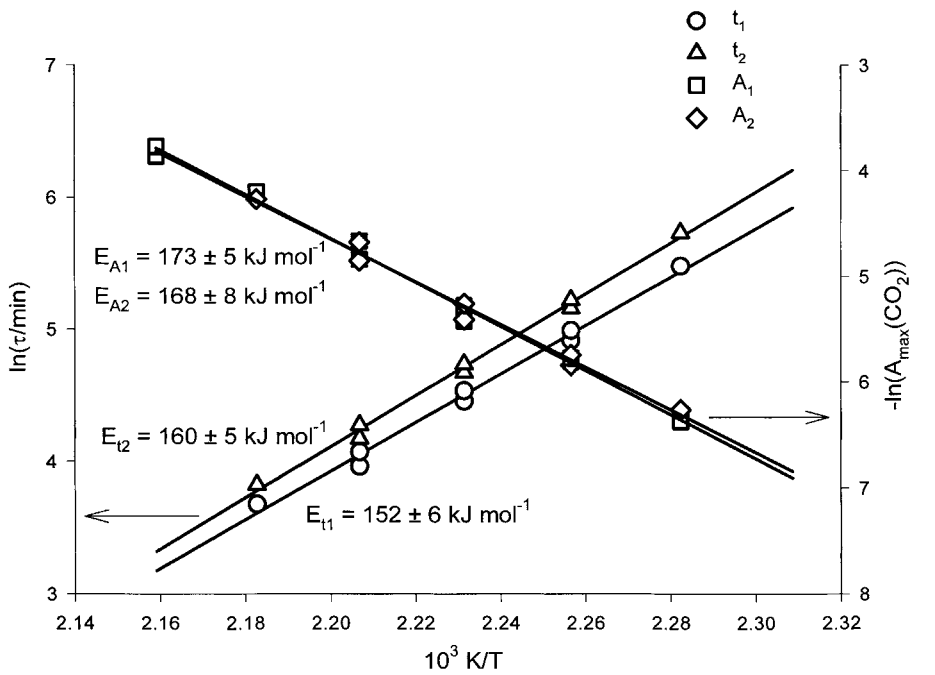

Fig. 7. Plot of time-to-event and CO_2 absorbance data for isothermal TG–DTA–FTIR–MS experiments for both KDNBF samples: t_1 and A_1 refer to the time to the first peak in the carbon dioxide absorbance, t_2 and A_2 to the second peak.

Table 3
Comparison of sensitivity data

Material	H_{50}/cm bureau of explosives impact	Limiting load/N BAM friction	ESD/J
Lead azide		0.1 [2]	
KDNBF	6.1 ± 1.3 (this work)	<5 (this work)	<0.006 (this work)
Mercury fulminate		5 [2]	
S/$KClO_3$ (30/70)	<4.2 (this work)	40 (this work)	
PETN	17 ± 4 (this work)	60 [2]	>0.156 (this work)
RDX	14 ± 3 (this work)	120 [2]	>0.156 (this work)

4. Discussion

4.1. Kinetic parameters, onset temperatures and energetics

It is clear from the multiple peaks in the DSC trace in Fig. 2 that the decomposition of KDNBF is not a single-step process. Implicit in any discussion of the decomposition is the fact that the overall process is complex, and that any rate parameters derived do not correspond to an elementary single step. Notwithstanding this, the phenomenological Arrhenius parameters can be used to estimate the overall rate constant for thermal decomposition for practical purposes.

The dynamic DSC experiments and the isothermal TG–DTA-FTIR-MS mass-loss curves were analyzed using the IsoKin isoconversional data analysis program [23]. The method allows activation energies to be extracted as a function of extent of reaction, α, and does not require assumptions to be made about the kinetic model for the reaction [24,25]. Only the initial stages of the reaction were considered. It was assumed that the end of the first peak in the DSC traces and the end of the initial steep mass loss (see Fig. 5) in the isothermal mass-loss experiments corresponded to $\alpha = 1.0$. The results are shown graphically in Fig. 8. The activation energies obtained for the two sets of data are in very good agreement over the range

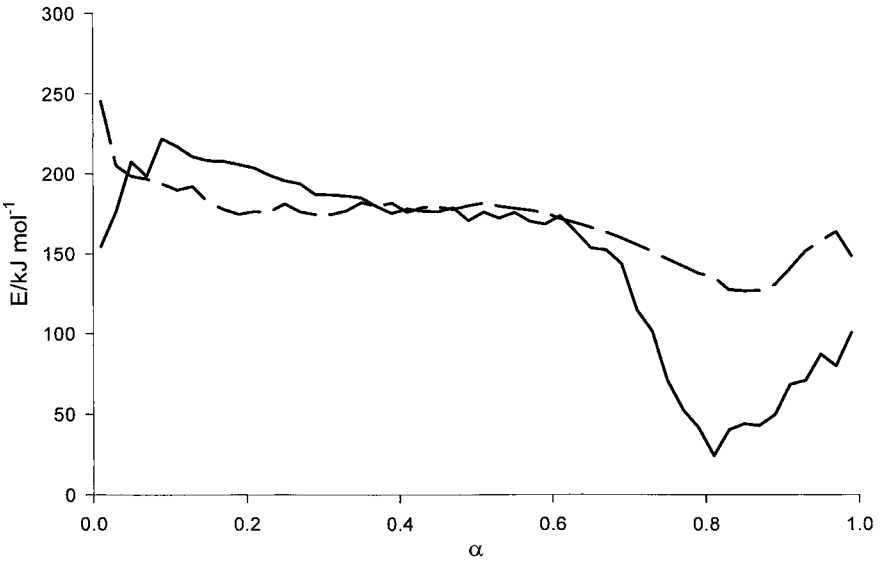

Fig. 8. Activation energy as a function of extent of reaction for the initial stages of KDNBF decomposition: dashed line, dynamic DSC data; solid line, mass-loss data from TG–DTA–FTIR–MS experiments.

Table 4
Comparison of kinetic parameters obtained for KDNBF using a variety of thermal techniques

Reference	Method	E/kJ mol^{-1}	ln/Z min^{-1}
[9]	TG isothermal, 3 mg vacuum continuously pumped, 363–423 K	126	32.0
[10]	DSC dynamic, 0.2 mg, 475–525 K (approximately), unsealed lids	179	43.2
[5]	TG dynamic, 1 mg, open-pan, 438–470 K, ASTM E1641	190 ± 6[a]	46.6 ± 0.3
[5]	TG isothermal, 1 mg, open-pan, 423–453 K, induction time	151 ± 2	–
[5]	TG isothermal, 1 mg, open-pan, 423–453 K, zero-order kinetics	173 ± 2	41.9 ± 0.6
[5]	ARC isothermal, 100 mg, closed bomb, 413–428 K, induction time	189 ± 6	–
[5]	Dynamic HFC, 10 mg, sealed ampoules, 438–477 K, ASTM E698	132 ± 4	31.4 ± 0.1[b]
This work	Dynamic DSC, 0.2 mg, unsealed lids, 470–494 K, ASTM E698	176 ± 5	42.7 ± 0.1
This work	Isothermal TG–DTA, 1 mg, open-pan, 438–463 K, time to first and second maxima in CO_2 production	152 ± 6, 160 ± 5	
This work	Isothermal TG–DTA, 1 mg, open-pan, 438–463 K, first and second peak rate of CO_2 production	173 ± 5, 168 ± 8	
This work	Isoconversional analysis of dynamic DSC measurements ($0.2 < \alpha < 0.6$)	178 ± 3	
This work	Isoconversional analysis of mass loss in isothermal TG–DTA experiments ($0.2 < \alpha < 0.6$)	181 ± 10	

[a] Quoted uncertainties refer to one standard deviation and experimental scatter only—no attempt is made to quantify the uncertainties inherent in each method.
[b] The pre-exponential factor quoted here is different from that previously published [5], owing to an error in the original data analysis.

$0.2 < \alpha < 0.6$. Averages over this range give E kJ mol^{-1} $= 178 \pm 3$ and 181 ± 10 for the dynamic DSC and isothermal mass-loss experiments, respectively, close to those found by other methods. The constancy of activation energy over this range of α suggests that the rate-limiting step is unchanged over most of the initial decomposition. Above $\alpha = 0.6$, the activation energies from the two set of data diverge, indicating that other processes are becoming important.

Kinetic parameters for the thermal decomposition of KDNBF, from our laboratory and elsewhere are summarized in Table 4. Arrhenius plots for the different studies where both Z and E were derived are shown in Fig. 9. For each case, rate constants are only plotted over the temperature range of the measurements. For studies where the temperature range is rather limited, small variations in the measured rate constants can make a big difference to the derived Arrhenius parameters. A comparison of rate constants is then often more meaningful than a comparison of Z and E.

The results previously obtained in our laboratory have been discussed in detail elsewhere [5]. Only two temperature-dependent studies from other laboratories are known to us. Whelan et al. [10] carried out similar dynamic DSC experiments to those reported on here, but at somewhat higher heating rates, with very similar results. They also reported that a 50 mg sample heated in a test tube at 5 °C min^{-1} ignited at 200 °C. Rouch and Maycock [9] carried out mass loss studies with a quartz spring balance apparatus between 90 and 150 °C, but encountered substantial experimental difficulties: they were only able to obtain consistent results when pumping continuously on the sample. They concluded that the results were perhaps affected by the presence of solvent occluded in the sample during the manufacturing process.

Very brief (one or two runs) DSC or DTA information has been published by Rouch and Maycock [9], Spear and Norris [14], Graybush et al. [11] and Hatano et al. [12]. It is difficult to compare peak temperatures, as these depend on the heating rate, sample size and other parameters, and the detailed experimental conditions are not always available from the original publications. In general, the peak temperatures observed by these authors are within a few degrees of those measured in the present study. The exception seems to be the work of Hatano et al., where peak temperatures of 182 and 184 °C were reported. The lowest peak temperature in the present study (at the slowest heating rate of 1 °C min^{-1}) was 197 °C. The reason for this discrepancy is not clear. In contrast, the average enthalpy of reaction 3.3 ± 0.4 kJ mol^{-1} measured in

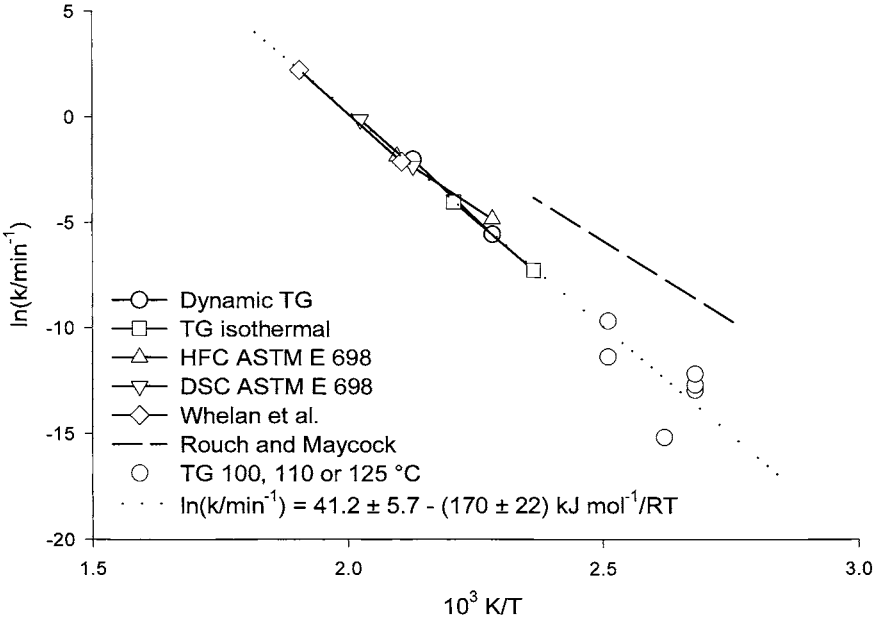

Fig. 9. Arrhenius plots for the thermal decomposition of KDNBF using different methods.

this work is in excellent agreement with the results of the two DSC runs reported by Hatano et al.

The agreement between the various measurements in Fig. 9 is excellent, with the exception of the results of Rouch and Maycock [9]. As discussed above, Rouch and Maycock experienced considerable experimental difficulties in taking measurements. An unweighted average of ln(Z) and E for the studies, where both Z and E were derived, excluding that of Rouch and Maycock, gives

$$\ln(k/\mathrm{min}^{-1}) = (41.2 \pm 5.7) - \frac{(170 \pm 22)\,\mathrm{kJ\,mol}^{-1}}{RT} \quad (1)$$

This expression is recommended for estimation of rate constants for KDNBF decomposition over the temperature range 350–550 K and is plotted in Fig. 9. The TG results from this work agree well with Eq. (1). Where activation energies alone were derived, these are also in very fair agreement with Eq. (1).

4.2. Mechanism of reaction

It is clear from the multi-step DSC and TG–DTA traces in the present work that the decomposition of KDNBF is a complex process. Earlier TG, DSC and DTA work in our laboratory [5] and elsewhere [9–14] confirms the complex nature of the decomposition.

The observation of a marked induction time in the present isothermal TG–DTA experiments and in previous isothermal TG and ARC experiments [5] strongly suggests that the decomposition of KDNBF is autocatalytic in nature. Alternatively, there could be an inhibition effect, with the inhibitor being consumed during the early stages of the reaction.

The thermal aging work described here clearly indicates that the properties of KDNBF depend on its thermal history. Although pre-heating the sample in the temperature range 150–180 °C produced the anticipated reduction of enthalpy change from the partially reacted sample, it also significantly reduced the onset temperature for thermal decomposition. We have observed similar behavior with nitrocellulose [26]. Rouch and Maycock [9] also observed a decrease in decomposition temperature with pre-heating: the DTA peak temperature was reduced by about 25 °C after KDNBF had been subjected to two cycles of 64 h "sterilization" in air at 125 °C. In contrast, no change in the DTA curve was observed after accelerated aging for 255 days at 86.1 °C. Using the Arrhenius parameters from the present DSC study, approximately 20% decomposition

would be expected during the pre-heating at 125 °C, compared to only 0.1% at 86.1 °C. It is possible that a certain level of decomposition is needed during the thermal aging process, in order to affect the measured onset temperature. This partial decomposition may either produce the reactive intermediates that give rise to autocatalysis, or consume an inhibitor.

Despite the complexity of the heat flow and mass loss curves, the products of the reaction are remarkably simple: carbon dioxide is the major product, accompanied by water and nitrous oxide. The time dependence and activation energy for the evolution of carbon dioxide agrees closely with that derived by DSC from heat flow measurements, indicating that carbon dioxide is produced in the main exothermic step.

The observation of carbon dioxide as a primary product underlines the fact that the decomposition is a multi-step process. There are no C–O bonds in the original molecule, so the production of carbon dioxide requires the breaking and forming of several chemical bonds. Similarly, there are no N–N bonds in the original molecule, so that production of nitrous oxide will necessarily be a multi-step process. The observation of cyanogen as a minor product is of interest, as there is a N–C–C–N linkage in the original molecule. Cyanogen is also highly toxic. Mass loss in both DSC and TG–DTA experiments in nitrogen or helium was approximately 60%, indicating the presence of a substantial solid residue. The solid residue was not subjected to a detailed analysis as part of the present work, but it is clearly carbon-containing, based on the evolution of carbon dioxide in TG–DTA experiments in air above 350 °C. A good deal more work would be required to elucidate the detailed mechanism of decomposition.

No significant variation in the peak temperature of the main exotherm was observed with pressure up to 6.89 MPa, or with confinement of the sample in a small glass ampoule [5]. Similarly, the kinetic results shown in Table 4 and Fig. 9 are very consistent, despite the fact that they were measured under widely varying conditions of confinement and free volume. These observations lead us to conclude that the initial decomposition is largely independent of pressure and the atmosphere above the sample.

No endotherm that could be associated with the melting of KDNBF was observed in the present DSC and DTA experiments. The significant decomposition of the material measured in the isothermal aging experiments demonstrates that a substantial part of the decomposition must take place from the solid phase. However, the strong initial exotherm could easily mask a melting endotherm and it is possible that some of the material is in a molten state at later stages of the reaction. In hot-stage microscopy experiments, Spear and Norris [14] observed that the crystals darkened, prior to melting and gas evolution, providing further evidence for this possibility.

4.3. Sensitivity

Based on the present results and those in the literature, KDNBF is an extremely sensitive material, as would be expected from a primary explosive. Positives in all tests were signaled by a violent reaction, presumably a detonation, together with total consumption of the product. Literature sensitivity values for KDNBF and other materials are compared to the present results in Table 3. It is well known that the results of sensitivity tests are very dependent on the apparatus and the experimental details. Table 3 only shows data collected using the same apparatus as used in the present study.

In experiments where different apparatus was used, the results are very consistent with the present work. Spear and Norris [14] found that KDNBF fires at their lowest energy of 45 mJ in ESD testing. They also observed that KDNBF was very impact sensitive, with 4/10 positives at 10 cm in their ball-and-disk test. Using an underwater gap test, Hatano et al. [13] determined that KDNBF is slightly more sensitive to shock than lead azide. In a separate publication, Hatano et al. [12] found that KDNBF and lead azide have similar impact sensitivities, based on a drop-ball test.

The sensitivity of KDNBF is considered to be between that of lead azide and that of mercury fulminate [1]. From the data in Table 3, this seems to be the case for friction stimuli. Not enough information is available to confirm whether the same holds for impact and ESD stimuli, using the present apparatus.

Acknowledgements

The authors would like to thank Professor C. Wight for generously providing a copy of the IsoKin program.

References

[1] B.T. Fedoroff, O.E. Sheffield, Encyclopedia of Explosives and Related Articles, Vol. 2, Picatinny Arsenal, Dover, NJ, USA, 1962.

[2] J. Kohler, R. Meyer, Explosives, 4th Revised and Extended Edition, VCH Publishers, Chichester, 1993.

[3] H.A. Scott, PCT International Patent Application WO 9914171, 25/03/99.

[4] G.B. Carter, Canadian Patent Application 2,156,974, 28/02/96.

[5] D.E.G. Jones, H.T. Feng, R.C. Fouchard, J. Thermal Anal. 60 (2000) 917.

[6] D.E.G. Jones, H.T. Feng, R.C. Fouchard, in: Proceedings of the 26th International Pyrotechnics Seminar, Nanjing, China, 1–4 October 1999.

[7] D.E.G. Jones, H.T. Feng, R.C. Fouchard, in: Proceedings of the NDIA Symposium on Insensitive Munitions and Energetic Materials Technology, San Diego, CA, USA, 16–19 November 1998.

[8] D.E.G. Jones, H.T. Feng, R.C. Fouchard, in: Proceedings of the 25th International Pyrotechnics Seminar, EUROPYRO 99, Brest, France, 7–11 June 1999.

[9] L.L. Rouch Jr., J.N. Maycock, NASA Contract Report, NASA CR-2622, 1976.

[10] D.J. Whelan, R.J. Spear, R.W. Read, Thermochim. Acta 80 (1984) 149.

[11] R.J. Graybush, F.G. May, A.C. Forsyth, Thermochim. Acta 2 (1971) 153.

[12] H. Hatano, F. Yoshizawa, H. Yabashi, Y. Wada, M. Tamura, F. Hosoay, T. Yoshida, Kogyo Kayaku 51 (1990) 70.

[13] H. Hatano, H. Yabashi, Y. Wada, T. Matsuzawa, F. Hosoya, M. Tamura, T. Yoshida, Kogyo Kayaku 51 (1990) 343.

[14] R.J. Spear, W.P. Norris, Propellants Explosives Pyrotech. 8 (1983) 85.

[15] ASTM E967-83, American Society for Testing, Materials, Philadelphia, PA, USA; ASTM E968-83, American Society for Testing, Materials, Philadelphia, PA, USA.

[16] ASTM E1582, American Society for Testing and Materials, Philadelphia, PA, USA.

[17] Test 3(a)(I) Bureau of Explosives Machine, Recommendations on the Transport of Dangerous Goods, Manual of Tests and Criteria, 2nd Revised Edition, United Nations, Geneva and New York, 1995.

[18] W. Dixon, A. Mood, J. Am. Stat. Assoc. (1948) 109.

[19] Test 3(b)(I) BAM Friction Apparatus, Recommendations on the Transport of Dangerous Goods, Manual of Tests and Criteria, 2nd Revised Edition, United Nations, Geneva and New York, 1995.

[20] D. Skinner, D. Olson, A. Block-Bolten, Propellants Explosives Pyrotech. 23 (1997) 34.

[21] ASTM E698, American Society for Testing and Materials, Philadelphia, PA, USA.

[22] R.L. Blaine, S.M. Marcus, J. Thermal Anal. 49 (1997)1485.

[23] IsoKin Isoconversional Data Analysis Program, Version 1.42, Copyright© 2000, Charles A. Wight, Center for Thermal Analysis, University of Utah.

[24] S. Vyazovkin, C.A. Wight, J. Phys. Chem. A 101 (1997) 5653.

[25] S. Vyazovkin, C.A. Wight, Chem. Mater. 11 (1999) 3386.

[26] D.E.G. Jones, unpublished results.